Figure 1   Determination of TRP for Ion Channels Associated With LQT1

(A) The 192-cell array used in the computational simulation of transmural repolarization prolongation (TRP) in patients with long QT syndrome type 1 (LQT1). Action potential determination for wild-type channels at the different cell types is shown. **(B)** Determination of pseudo-transmural electrocardiography (ECG) based on the wild-type channel action potential duration across the array of cells. **(C)** Pseudo-transmural ECG simulated for mutant channels in the study with lower **(left)** and higher **(right)** prolongation observed. A unique TRP parameter was determined for each mutant ion channel as indicated. **(D)** Correlation of TRP determined from simulation with patient QT interval corrected for heart rate (QTc) for all patients genotype positive for each mutation. **(E)** Location of mutations in the study. Mutations associated with the top quartile TRP are marked in **red. Circle size** indicates number of patients with the mutation.

Upon enrollment in the registry, clinical history was obtained; thus follow-up data in the current study comprised historical data from birth to enrollment and prospective information collected at yearly intervals after enrollment. The mean age at enrollment in the registry among the patients from the Rochester registry (77% of the patients studied) was 26 years, and follow-up for the survival analysis was from birth through age 40 years. On average, 69% of the follow-up data were obtained retrospectively at enrollment. Only patients for whom a complete medical history and prospective information were available were included in the present study. Clinical history data were collected on forms and included demographic characteristics, personal and family medical history, ECG findings, medical therapies, left cardiac sympathetic denervation, implantation of a pacemaker or an implantable cardioverter defibrillator (ICD), and the occurrence of LQTS-related cardiac events.

LQTS-related cardiac events included *syncope*, defined as transient loss of consciousness abrupt in onset and offset, ACA requiring defibrillation, and SCD without a known cause. Each subject had a single individual QTc value assigned, obtained at the time of entry in the LQT registry. **Genotyping.** The *KCNQ1* mutations were identified with the use genetic tests performed in academic molecular-genetic laboratories, including the Functional Genomics Center, University of Rochester Medical Center, Rochester, New York; Baylor College of Medicine, Houston, Texas; Mayo Clinic College of Medicine, Rochester, Minnesota; Boston Children's Hospital, Boston, Massachusetts; Laboratory of Molecular Genetics, National Cardiovascular Center, Suita, Japan; Department of Clinical Genetics, Academic Medical Center, Amsterdam, The Netherlands; and Statens Serum Institut, Copenhagen, Denmark. For the proband in each family, the 5 most common LQT loci (*KCNQ1, KCNH2, SCN5A, KCNE1,* and *KCNE2*) were fully sequenced to identify the mutation by comparing the sequence with those of healthy individuals without LQTS. Once a mutation was identified in other family members, and the *KCNQ1* gene was sequenced to confirm the presence or absence of the mutation.

Specifically, after informed consent was obtained, blood samples from patients were sent for detailed mutational analysis involving either 12 LQTS genes (*KCNQ1, KCNH2, SCN5A, ANK2, KCNE1, KCNE2, CACNA1C, KCNJ2, CAV3, SCN4B, AKAP9,* and *SNTA1*) or 5 LQTS genes (*KCNQ1, KCNH2, SCN5A, KCNE1,* and *KCNE2*) and were screened for multiple LQTS mutations/polymorphisms. Genetic tests included next-generation DNA sequencing of all of the coding exons. For that, exons and adjacent splice sites of each of the genes were sequenced using a solid-state sequencing-by-synthesis process (Illumina, Inc., San Diego, California). There are over 230 exons to be sequenced in LQTS; 12 gene panels and both alleles of each exon (maternal and paternal) were sequenced simultaneously. Polymerase chain reaction primers flanking each exon of the regions of interest were designed to generate amplicons ranging in size from ~200 to 600 bp, avoiding any nonunique sequences, as well as positions of known polymorphisms and mutations. The products of all multiplex reactions for a specific patient were pooled. Sequencing itself first required cluster generation, which is the process of attaching individual fragments from a patient's library to a chambered glass slide and replicating them in situ to produce distinct islands of homogeneous fragments. Using the Genome Analyzer II (Illumina, Inc.), sequencing-by-synthesis chemistry was performed in the slide chambers to which the clusters were attached. Each base (A, C, G, or T) added to a growing DNA strand liberates 1 of 4 associated fluorochromes in a local reaction that was captured by photoimaging cycle for each cluster. Photoimaged data from each cluster of molecules were converted to base calls and aligned to a reference sequence for each gene of interest using Illumina-provided software. Various annotation databases (e.g., dbSNP, HGMD, and the rapidly growing local compilations) were used, when possible, to classify nucleotide differences into various categories, ranging from polymorphisms to pathogenic mutations.

Electrophysiology. The electrophysiologic properties of mutant *KCNQ1* channels were obtained by overexpression in *Xenopus laevis* oocytes as previously described (8,17,18). Experiments were performed in cells expressing WT human *KCNQ1* (NP_000209.2) and WT human *KCNE1* (NP_001121142). Mutations were generated by polymerase chain reaction–based site direct mutagenesis of the WT *KCNQ1* construct, using PFU ultra DNA polymerase and construct sequences confirmed by DNA sequencing. The average measurement of at least 18 cells expressing mutant channels were used to determine changes in ion channel parameters compared to WT channels. Thus, the same *KCNQ1* source was used for all of the mutant ion channels, with the only difference being the mutation specified in the study. All mutations analyzed for TRP were present among study subjects.

In brief, WT and mutant *KCNQ1* cRNA were injected into oocytes in a 1:1 ratio, together with the *KCNE1* subunit (0.5:0.5:1 ratio *WTKCNQ1:MutKCNQ1:KCNE1*). The IKs tail current at −40 mV was measured after depolarization to a series of voltage steps from −50 to +80 mV every 10 mV, and a Boltzmann fit ($G = g_{max}/(1 + \exp[-(V - V_{1/2})/k]$) of these data was used to determine the steepness or slope factor (k), the voltage that elicits half of the maximal activation ($V_{1/2}$) of activation, and the maximal conductance (g_{max}). Nonsense mutation effects were assumed to have had a haploinsufficient phenotype, and effects were evaluated by measuring currents with decreased WT expression (0.5:1 ratio *WTKCNQ1:KCNE1*).

Statistics. Linear regression was used to test for correlation between simulated repolarization time using the model described above and QTc measured from patients. Kaplan-Meier survival analysis was used to determine the cumulative probability of cardiac events by simulated repolarization

times and by measured QTc interval, and significance was tested by the log-rank test. Multivariate Cox proportional hazards regression modeling was used to evaluate the independent contribution of simulated repolarization times to the occurrence of cardiac events from birth through age 40 years. Additional prespecified covariates in the multivariate models included sex, the patient's individual QTc, and time-dependent beta-blocker therapy (i.e., by taking into account in the multivariate model's information regarding administration of beta-blockers given to patients at different time points during follow-up). Patients who did not have an ECG for QTc measurement (n = 92) were identified in the Cox models as "QTc missing," and all Cox models were adjusted for this missing QTc parameter. Data from the International LQTS Registry demonstrated that an age-interaction existed regarding the effect of sex and genotype on the occurrence of cardiac events, with a crossover effect for both genotype and sex after the onset of adolescence (5,19). During childhood, the risk for cardiac events is significant higher in boys with LQTS, in particular LQT1 (5,19–21). Therefore, to avoid a violation of the proportional-hazards assumption, models were carried out using a time-dependent covariate for sex with prespecified younger males (ages 0 through 13 years) and older females (ages 14 through 40 years), allowing for different hazard ratios by sex before and after adolescence.

Because almost all of the patients were first- and second-degree relatives of probands, the effect of lack of independence between patients was evaluated in the Cox model, with grouped jackknife estimates for family membership (9). All grouped jackknife standard errors for the covariate risk factors fell within 3% of those obtained from the unadjusted Cox model, and therefore only the Cox model findings are reported. The statistical software used for the analyses was SAS version 9.20 (SAS Institute Inc., Cary, North Carolina). A 2-sided 0.05 significance level was used for hypothesis testing.

Results

Simulation of transmural repolarization time. Simulation of transmural ECGs was performed for each of the mutants using mutant basic electrophysiological characteristics as previously determined (8), producing the simulated transmural electrical potentials shown in Figures 1A and 1B. The change in simulated transmural repolarization time for mutant channels compared to WT is referred to as the *TRP. Transmural repolarization* was defined as the difference of WT and mutant pseudo-transmural QT measured at the end of the T wave. The maximal slope intercept method was used, defining the end of the T wave as the intercept between the isoelectric line with the tangent drawn through the maximum down slope of the T wave (Fig. 1C). TRP values associated with each mutant channel are shown in Figures 1A and 1D. For one of the mutant channels tested (*D611Y*), repolarization time was predicted

Table 1   Characteristics of the Study Population

Characteristic	TRP		p Value
	Upper Quartile (n = 186)	Lower Quartiles (n = 447)	
ECG parameters			
Overall QTc, ms	502 ± 53	475 ± 49	<0.001
QTc >500 ms	49	26	<0.001
RR, ms	804 ± 232	847 ± 200	0.04
LQTS therapies during follow-up			
Beta blockers	47	44	0.49
Pacemaker	1.1	2.2	0.49
ICD	6	8	0.39
Cardiac events during follow-up			
Syncope	59	29	<0.001
ACA, %	7	2	0.007
SCD	18	7	<0.001
Appropriate ICD shocks	0	0.2	
ACA or SCD*	23	9	<0.001
Race			
Caucasian	69.5	80	<0.001
Asian	2	12	<0.001
Other	0.5	0	
Unknown†	28	8	<0.001

Values are mean ± SD or %. *Only the first event for each patient was considered. †Patients of unknown race from Northern European Registries, likely Caucasian.

ACA = aborted cardiac arrest; ICD = implantable cardioverter defibrillator; LCSD = left cervical sympathetic denervation; MS = membrane spanning domain; SCD = sudden cardiac death.

to be shorter (−7 ms) than the one produced by the presence of the WT channel, while other mutations caused changes ranging from +4 ms (*R591H*) to +49 ms (*G314S*). The mean TRP for all mutations was 27.5 ms. Mutations with the largest effects on TRP (top quartile [>36 ms]) were present in the transmembrane domain of the channel—1 in the S4-S5 cytoplasmic loop (*V254M*), 1 in the S5 membrane spanning domain (*L266P*), and 2 in the pore loop (*T312I* and *G314S*). Figure 1E shows the KCNQ1 channel protein with the location of the mutations in the study population. Mutations resulting in TRP in the top quartile are shown in red, and others are shown in green.

Baseline patient characteristics by TRP. A simulated value of prolonged transmural repolarization (TRP upper quartile) among all mutations studied was present in 186 patients (29%). The mean QTc of these patients was 502 ± 53 ms, significantly prolonged compared to patients with a simulated lower quartiles TRP (475 ± 49 ms; p < 0.001). Other baseline characteristics of patients with upper quartile TRP are shown in Table 1, demonstrating no significant difference in heart rate (RR interval), sex, or beta-blocker usage among patients with a prolonged TRP. In addition, patients with upper quartile TRP had a higher frequency of cardiac events during follow-up, including syncope, ACA, and SCD (Table 1).

Correlation between TRP and measured QTc. To measure the correlation between TRP and individual patient QTc, TRP for each patient was plotted against the patients' measured baseline QTc (Fig. 1D). This plot illustrates the

broad variation in QTc measurements from patients with the same mutation. Simple linear regression (shown as red solid line), demonstrates a weak association between QTc and TRP (R = 0.27; p < 0.0001). Although the values were correlated, there was a wide distribution of individual QTcs for each modeled mutation. The baseline QTc measurements variation among patients with the same IKs mutation also was consistent with the significant variation observed among multiple measurements taken from a single individual (7). The correlation coefficient (R^2) for a linear correlation between individual QTc for all patients and mean QTc for patients with each mutation was 0.11 (Online Fig. 4A), suggesting that QTc variability among individuals shows, as TRP, a weak correlation with QTc variability. These results suggest that modeled TRP values predicted the ion channel mutation–specific contribution of cardiac risk. Consistent with TRP explaining a population variability of QTc, TRP showed a reasonable correlation with the mean QTc in a population with the same mutation (TRP vs. mean QTc for all patients with each mutation; R^2 = 0.35) (Online Fig. 4B). In addition, to estimate individual QTc variability, data from 10 patients in whom a large number of QTc determinations was available were examined (these data were not included in the primary study). These patients showed an average QTc standard deviation of (39 ± 1 ms) (Online Fig. 5), similar to that found among patients with the same mutation (39 ± 2 ms) (Online Fig. 5), suggesting that QTc variability may reflect, in large, variability observed in the individual patient over time. Because of this inherent variability in QTc determination, deterministic modeling results, such as TRP, may provide a clearer signal that can be used to evaluate risk in the patient.

TRP is an independent risk factor for cardiac events in LQT1. In a multivariate Cox regression model, mutant-specific TRP was significantly associated with an increased rate of cardiac events both as a continuous and as a dichotomized variable independent from other clinical variables and after adjustment for the patient's individual QTc (Table 2). For every additional 10-ms increment in simulated TRP, there was a corresponding significant 35% (p < 0.001) increase risk for the occurrence of cardiac events. Kaplan-Meier survival analysis with 4 subclassifications of TRP showed that the top quartile of TRP has an increased cumulative probability of cardiac events compared to those of the 3 lower quartiles (Online Fig. 6), indicating that probability of cardiac events is associated with a threshold level of TRP. In patients with mutations identified to have upper quartile with a simulated TRP, the risk for cardiac events was increased nearly 3-fold (p < 0.001). Consistent with these findings, Kaplan-Meier survival analysis (Fig. 2A, middle panel) showed that the cumulative probability of cardiac events from birth through age 40 years was significantly higher among patients with upper quartile simulated TRP compared with patients with lower TRP values. The population in the International Long QT Registry is estimated to be approximately 90% Caucasian.

Table 2	Multivariate Analysis: Risk Factors for Cardiac Events (Syncope, Sudden Death, and Aborted Cardiac Arrest) Among Patients With LQT1*		
Parameter	**Hazard Ratio**	**95% CI**	**p Value**
TRP assessed as a continuous measure			
TRP per 10 ms	1.35	1.18–1.56	<0.001
QTc ≥500 ms vs. <500 ms	1.78	1.34–2.38	<0.001
Male age ≤13 years	1.58	1.16–2.14	0.003
Female age ≥14 years	1.47	0.98–2.19	0.06
Time-dependent β-blocker	0.37	0.20–0.66	<0.001
TRP dichotomized at the upper quartile			
TRP Q4 vs. Q1–3	2.80	1.96–4.01	<0.001
QTc ≥500 ms vs. <500 ms	1.78	1.37–2.32	<0.001
Male age ≤13 years	1.60	1.19–2.15	0.002
Female age ≥14 years	1.38	0.91–2.09	0.13
Time dependent β-blocker	0.32	0.18–0.58	<0.001

*Multivariate analysis was carried out using Cox proportional hazards regression modeling; separate models were developed for each analysis, with adjustments for the 5 covariates in each part.

LQT1 = long QT syndrome type 1; QTc = QT interval corrected for heart rate; TRP = simulated pseudo-transmural electrocardiographic prolongation.

Asian race is underrepresented in the high quartile TRP (Table 1); nonetheless, when race was included in the models, it did not predict outcome, and the effect of TRP was similar.

Simulation of transmural ECG prolongation as an independent risk factor for cardiac events in LQT1 in patient with QTc <500 ms. In a secondary analysis, risk factors for cardiac events were evaluated among patients with only mild to moderate QTc prolongation (<500 ms) because, in this patient subset, individual QTc provides less prognostic information. Among these patients, each additional 10 ms of simulated TRP was associated with a significant 36% (p < 0.001) increased risk for cardiac events (Table 3). Upper quartile TRP was associated with nearly a 3-fold increased risk (2.97; 95% CI: 2.00 to 4.40) after adjustment for patients' individual QTc. Consistent with these findings, Kaplan-Meier curves including only patients with QTc <500 ms demonstrated early separation of event-free survival rates when patients were grouped into the upper versus lower TRP quartiles (Fig. 2B). When patients were stratified by both individual baseline QTc and TRP, Kaplan-Meier survival analysis showed that the group with upper TRP had a significantly higher event rate throughout follow-up, regardless of patients' individual QTc (Fig. 2C). Results from multivariate Cox proportional hazard regression analysis corresponding to the groups in Figure 2C are shown in Online Table 2.

To test whether TRP simulation parameters further improved clinical risk stratification compared with previously identified risk factors related to ion channel characteristics, secondary analysis added slow rate of channel activation as a covariate. Previous work showed that that channels with slow rates of activation (over 20% slower than WT channels) were associated with an increased risk for cardiac events (8). The results showed that for both the
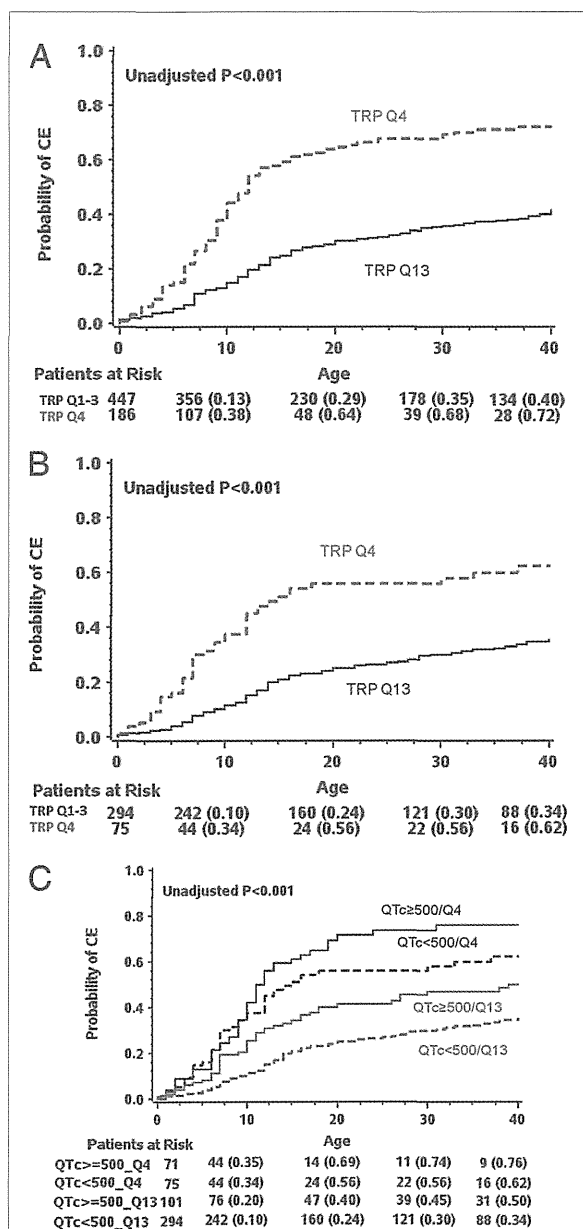
Figure 2   Rate of Cardiac Event During Follow-Up

Cumulative probability of the first cardiac event (syncope, aborted cardiac arrest, or death) during follow-up, dichotomized by patients with the highest quartile TRP (Q4) and all other quartiles (Q1–3) **(A)** among all study patients; **(B)** among the subset of patients with QTc <500 ms; **(C)** among all patients with combined assessment of TRP and QTc. Abbreviations as in Figure 1.

population as a whole and for patients with QTc <500 ms, slower channel activation and TRP top quartile were independent risk factors (Table 3). Additionally, because QTc ≥480 ms was found to be a very poor predictor of event risk in this population (hazard ratio [HR]: 0.96; 95% CI: 0.63 to

1.46; p = 0.85), a secondary analysis evaluated the association between QTc ≥450 ms and event risk in this population. This lower threshold was a similarly poor predictor of risk (HR: 1.09; 95% CI: 0.71 to 1.67; p = 0.71) (Online Table 3).

Simulation of transmural ECG prolongation as an independent risk factor for life-threatening cardiac events (ACA/SCD) in LQT1. In a multivariate Cox regression model, mutation-specific TRP was also significantly associated with an increased risk for live-threatening cardiac events (defined as first occurrence of ACA or SCD). The risk for ACA/SCD associated with TRP was consistent when this parameter was assessed as both a continuous measure and dichotomized at the upper quartile (>36 ms), after adjustment for individual patients' QTc (Table 4). Thus, for every additional 10 ms of added simulated transmural repolarization time, there was a corresponding significant 37% increase in the risk for ACA/SCD. Furthermore, the group carrying a mutation with upper quartile TRP had a >2-fold (p = 0.002) increased risk for ACA/SCD after adjustment for the individual patients' QTc (Table 5). This is also illustrated by Kaplan-Meier curves (Fig. 3), with early separation of event-free survival rates for the population of patients with upper quartile TRP.

Discussion

This study describes a method of simulating transmural myocardial repolarization based on WT and mutant channel characteristics determined in cellular electrophysiology. This transmural repolarization parameter was found to be an independent predictor for the occurrence of cardiac events and life-threatening events in patients with LQT1. The risk associated with simulated TRP was shown to be independent of patients' baseline QTc. These results regarding mutation-specific risk are particularly important for the subpopulation with mild to moderate QTc prolongation

Table 3	Multivariate Analysis: Risk Factors for Cardiac Events (Syncope, Sudden Death and Aborted Cardiac Arrest) Among 369 patients with LQT1 and QTc <500 ms		
Parameter	Hazard Ratio	95% CI	p Value
TRP assessed as a continuous measure			
TRP per 10 ms	1.36	1.18–1.56	<0.001
QTc ≥480 ms vs. <480 ms	0.99	0.67–1.46	0.97
Male aged ≤13 years	1.42	0.87–2.33	0.16
Female aged ≥14 years	1.86	0.96–3.60	0.06
Time-dependent β-blocker	0.48	0.23–1.02	0.06
TRP dichotomized at the upper quartile			
TRP Q4 vs. Q1–3	2.97	2.00–4.40	<0.001
QTc ≥480 ms vs. <480 ms	0.96	0.63–1.46	0.85
Male aged ≤13 years	1.38	0.86–2.21	0.19
Female aged ≥14 years	1.90	0.98–3.67	0.06
Time dependent β-blocker	0.45	0.22–0.58	0.04

Abbreviations as in Table 2.

Table 4	Multivariate Analysis: Risk Factors for Cardiac Events (Syncope, Sudden Death and Aborted Cardiac Arrest)*		
Parameter	Hazard Ratio	95% CI	p Value
TRP dichotomized at the upper quartile for the whole population			
TRP Q4 vs. Q1–3	2.25	1.49–3.39	<0.001
τ_{act} >1.20	1.42	1.00–2.03	0.05
QTc ≥500 ms vs. <500 ms	1.73	1.32–2.27	<0.001
Male aged ≤13 years	1.60	1.17–2.18	0.003
Female aged ≥14 years	1.39	0.981–2.11	0.12
Time dependent β-blocker	0.33	0.18–0.59	<0.001
TRP dichotomized at the upper quartile for patients with QTc <500 ms			
TRP Q4 vs. Q1–3	2.11	1.23–3.61	<0.01
τ_{act} >1.20	1.70	1.03–2.80	0.04
QTc ≥480 ms vs. <480 ms	0.94	0.62–1.43	0.78
Male aged ≤13 years	1.39	0.84–2.28	0.19
Female aged ≥14 years	1.86	0.95–3.65	0.07
Time dependent β-blocker	0.44	0.21–0.92	0.03

*Multivariate analysis was carried out using Cox proportional hazards regression modeling; separate models were developed for each analysis, with adjustments for the covariates in each part.
Abbreviations as in Table 2.

| Figure 3 | Rates of Life-Threatening Cardiac Events During Follow-Up |

Cumulative probability of aborted cardiac arrest or sudden cardiac death during follow-up among all study patients, dichotomized by patients with the highest quartile TRP (Q4) and all other quartiles (Q1–3). Abbreviations as in Figure 1.

(QTc <500 ms), in whom clinical risk factors provide less prognostic value. This report shows cardiac modeling being used as an arrhythmic risk predictor validated against a patient population in clinical practice.

Several experimental and computation models have been developed on the premise that transmural ECGs are a surrogate for the QT interval as measured by body surface ECGs. Transmural repolarizations are also thought to be particularly important in generating inhomogeneities of repolarization that lead to cardiac arrhythmias (22,23). IKs channel expression changes across the ventricular wall, contributing to transmural dispersion of repolarization (24–26). This is consistent with the present results, which indicate a significant increase in cardiac risk associated with mutation-

Table 5	Multivariate Analysis: Risk Factors for SCD/ACA Among All Patients With LQT1*		
Parameter	Hazard Ratio	95% CI	p Value
TRP used as a continuous variable			
TRP per 10-ms increment	1.27	1.02–1.59	0.03
QTc ≥500 ms	3.93	1.96–7.87	<0.001
Male age ≤13 years	2.16	1.22–3.84	0.008
Female age ≥14 years	1.19	0.63–2.26	0.59
Time dependent β-blocker	0.40	0.16–0.98	0.046
TRP dichotomized at top quartile			
TRP Q4 vs. Q1–3	2.24	1.96–4.01	0.002
QTc ≥500 ms vs. <500 ms	3.95	1.37–2.32	<0.001
Male age ≤13 years	2.24	1.19–2.15	0.005
Female age ≥14 years	1.12	0.91–2.09	0.74
Time dependent β-blocker	0.38	0.15–0.94	0.04

*Multivariate analysis was carried out using Cox proportional hazards regression modeling; separate models were developed for each analysis, adjusting for the 5 covariates in each part.
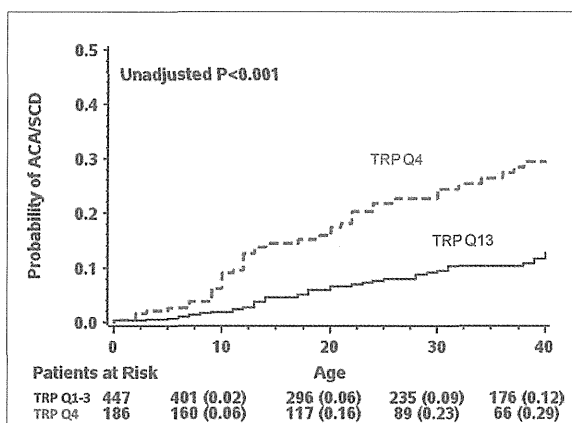Abbreviations as in Table 2.

specific changes in IKs and transmural repolarization in LQT1. In these models, the action potential duration dispersion can produce conditions to support reentrant activation patterns. Future, more detailed studies of arrhythmia mechanisms modeling higher dimensional tissue structure that can support a reentrant activation pattern are necessary. In addition, the use of TRP as an index for cardiac risk in other inherited and acquired LQT syndromes is promising but needs further study.

The authors showed previously that a slow activation rate is an independent risk factor in LQT1. The results indicate that TRP is independent from channel slow activation rate. Notable is that all 4 mutant channels in the top quartile of TRP show also slow activation kinetics (8). Nonetheless, TRP combines slower activation, changes in voltage dependence of activation, and conductance of the channel in relevant cardiac cell types to provide an overall effect of the mutation regarding transmural repolarization. This utilizes information on ion channel distribution and consequences of ion channel dysfunction for APD and propagation across the myocardial wall. Using this novel method, 4 high-risk mutations were identified, only 1 of which had been identified in the previous study. Most important, the present study showed that these high-risk mutations predicted life-threatening arrhythmic risk in the study population.

The simulation model proposed here consists of electrically coupled cardiac cells with heterogeneous electrophysiologic properties that produce waveforms that are similar to those measured experimentally (27–29). The development of heterogeneous models depends both on accurately representing the AP of the different cell populations and realistic coupling between the cells. At the single cell level, the exact difference in membrane currents and Ca^{2+} handling that produce differences across the ventricular wall is

controversial and very likely both region and species dependent. On the basis of the 3 standard cell types (epi-, endo-, and midmyocardial) in Flaim et al. (14), parameters were continually varied to interpolate differences in IKs, transient outward potassium current (I_{to}), I_{NaL}, and Ca^{2+} handling in an attempt to match the experimentally measured transmural profiles (28). The conductivity between cells was assumed to have been fixed, so that the conduction velocity was constant across the ventricular wall, as seen experimentally (28,30). This assumption of constant conductivity is consistent with the limited available experimental data that show that resistance is uniform, with the exception of a layer with higher resistivity (29). This layer, situated to roughly 30% depth, involves a systematic change in cellular orientation. The discontinuity in cellular orientation cannot be directly represented in the 192 equally spaced point models comprising our 1-D cable. However, future extensions to the model could incorporate this additional level of detail.

A recent study (31) used Markov models, AP and transmural ECG simulations to infer the mechanism of arrhythmia generation associated with a LQT1 associated mutation present in 1 patient with normal QTc and a history of syncope (*Q357R*, not included in the present study). The predisposition to arrhythmia was demonstrated by the propensity to generate early after depolarization (EADs) when combined with IKr blockage and beta-adrenergic drive, whereas the effect on the simulated TRP alone (without IKr blockage and beta-adrenergic drive) was mild (13 ms). This TRP value is comparable to the ones associated with mutations in this study with TRP in the first quartile, a range associated with 35% risk for a cardiac event by age 40 years. In contrast to the previous study, the present study focuses on how TRP relates to a clinical risk that may be revealed over the time frame of up to 40 years for a patient population. Because the present study included a large number of mutations, we chose a simpler Hodgkin-Huxley model of IKs that could be systematically constrained by the in vitro data. Although Markov models can potentially capture additional mechanistic details of ion channel function, identification of states and constraining parameters are difficult and complex with typical electrophysiologic data (32).

Simulated repolarization prolongation weakly correlated with baseline QTc measurements in the study population, which supports physiologic relevance of the simulation method. However, QTc measurements can vary widely among patients with a particular mutation and over time in the same patient (7). In addition, QTc has been shown to change during exercise (33) and with age (5) and has been suggested to depend on a patient's emotional state (34). The simulated transmural repolarization parameter described here may reflect an overall lifetime risk in patients with each specific mutation, a risk that may not be reflected in a single determination of patients' QTc. A reasonable correlation was found between the TRP and the mean QTc in a population with the same genotype, suggesting that deter-

ministic modeling results may provide a clearer signal than patient data with high variability and stochastic effects. Other genetic factors (e.g., SNPs in ion channels, modifier protein, and receptors) and unknown functional effect of the mutations, such as a decrease in beta-adrenergic activation (35), that are not taken into account in the TRP modeling, may also influence individual patients' QTc and/or risk for cardiac arrhythmias, with the possibility of both influencing or masking genotype-specific cardiac risk.

Here, mutations associated with high risk for cardiac events were identified in patients with LQT1. Four of these mutations, the ones included in the top quartile of repolarization dysfunction, were identified as being of particularly high risk: *V254M, L266P, T312I,* and *G314S.* These are all highly conserved residues among voltage-gated potassium channels, suggesting an important physiologic role (8,36). The authors recently showed that *V254M* has impaired beta-adrenergic activation, which would contribute to an increase in risk in patients with this mutation at high adrenergic states; the other mutations were not identified previously as being of particularly high risk.

Study limitations. Although the present findings regarding the use of simulated TRP in risk stratification are novel, these results are based on a single-population study of 633 patients with LQT1, and therefore need to be further validated in larger populations, comprising also patients with recently identified novel mutations in the *KCNQ1* gene. Partly retrospective data collection has limitations. However, because this is an analysis of registry data of a rare disease (in which a prospective clinical trial or an analysis of events from birth would be difficult), the authors believe that this type of analysis is the best way to handle the survival bias conferred by entering the registry at an older age and the exclusion of higher-risk patients who died at a younger age. The present study attempted to identify the incremental prognostic implications of computed modeling of electrophysiologic modeling in LQTS, but did not investigate the reason why the model TRP is a good risk predictor. For this, higher-dimensional tissue structure that can support a re-entrant activation pattern is necessary.

Conclusions

The identification of mutations conferring a high risk for cardiac events can help to guide treatment decisions by identifying those patients who will benefit most from therapies including pharmacologic agents (i.e., beta-blockers) and implantable defibrillators. In particular, patients with moderate QTc prolongation (i.e., QTc <500 ms) are a challenge for clinicians because their risk for cardiac events remains significantly elevated compared to that of the general population, although the markers of risk are relatively unknown (9). We have shown that simulated TRP is a particularly strong marker of risk for cardiac events in this population, which may translate into changes in treatment decisions for identifying high-risk LQTS patients

independently of traditional ECG markers. It would be recommended that patients with the identified prolonged TRP mutations (*V254M, G314S, T312I,* and *L266P*) should be considered to be at a high risk for cardiac events even in the absence of QTc prolongation or other clinical risk factors. This patient subset should be routinely treated with beta-blocker therapy at the maximal tolerated dosage and carefully followed up for residual symptoms during medical therapy.

Reprint requests and correspondence: Dr. Coeli M. Lopes, Department of Medicine, Box CVRI, Aab Cardiovascular Research Institute, University of Rochester School of Medicine & Dentistry, 601 Elmwood Avenue, Rochester, New York 14642. E-mail: Coeli_Lopes@URMC.Rochester.edu OR Dr. Ilan Goldenberg, Heart Research Follow-up Program, Box 653, University of Rochester Medical Center, Rochester, New York 14642. E-mail: Ilan.Goldenberg@heart.rochester.edu.

REFERENCES

1. Keating MT, Sanguinetti MC. Molecular and cellular mechanisms of cardiac arrhythmias. Cell 2001;104:569–80.
2. Hedley PL, Jorgensen P, Schlamowitz S, et al. The genetic basis of long QT and short QT syndromes: a mutation update. Hum Mutat 2009;30:1486–511.
3. Moss AJ. Long QT syndrome. JAMA 2003;289:2041–4.
4. Moss AJ, Shimizu W, Wilde AAM, et al. Clinical aspects of type-1 long-QT syndrome by location, coding type, and biophysical function of mutations involving the KCNQ1 gene. Circulation 2007;115:2481–9.
5. Zareba W, Moss AJ, Locati EH, et al. Modulating effects of age and gender on the clinical course of long QT syndrome by genotype. J Am Coll Cardiol 2003;42:103–9.
6. Priori SG, Napolitano C, Schwartz PJ, et al. Association of long QT syndrome loci and cardiac events among patients treated with beta-blockers. JAMA 2004;292:1341–4.
7. Goldenberg I, Mathew J, Moss AJ, et al. Corrected QT variability in serial electrocardiograms in long QT syndrome: the importance of the maximum corrected QT for risk stratification. J Am Coll Cardiol 2006;48:1047–52.
8. Jons C, Uchi J, Moss AJ, et al. Use of mutant-specific ion channel characteristics for risk stratification of long QT syndrome patients. Sci Transl Med 2011;3:76ra28.
9. Goldenberg I, Horr S, Moss AJ, et al. Risk for life-threatening cardiac events in patients with genotype-confirmed long-QT syndrome and normal-range corrected QT intervals. J Am Coll Cardiol 2011;57:51–9.
10. Horr S, Goldenberg I, Moss AJ, et al. Ion channel mechanisms related to sudden cardiac death in phenotype-negative long-QT syndrome genotype-phenotype correlations of the KCNQ1(S349W) mutation. J Cardiovasc Electrophysiol 2011;22:193–200.
11. Bianchi L, Priori SG, Napolitano C, et al. Mechanisms of I-Ks suppression in LQT1 mutants Am J Physiology-Heart Circ Physiol 2000;279:H3003–11.
12. Murray A, Potet F, Bellocq C, et al. Mutation in KCNQ1 that has both recessive and dominant characteristics. J Med Genet 2002;39:681–5.
13. Wang Z, Tristani-Firouzi M, Xu Q, Lin M, Keating MT, Sanguinetti MC. Functional effects of mutations in KvLQT1 that cause long QT syndrome. J Cardiovasc Electrophysiol 1999;10:817–26.
14. Flaim SN, Giles WR, McCulloch AD. Contributions of sustained I-Na and I-Kv43 to transmural heterogeneity of early repolarization and arrhythmogenesis in canine left ventricular myocytes. Am J Physiol-Heart Circ Physiol 2006;291:H2617–29.
15. Narayan SM, Bayer JD, Lalani G, Trayanova NA. Action potential dynamics explain arrhythmic vulnerability in human heart failure. J Am Coll Cardiol 2008;52:1782–92.
16. Keller DU, Seemann G, Weiss DL, Farina D, Zehelein J, Dossel O. Computer based modeling of the congenital long-QT 2 syndrome in the Visible Man torso: from genes to ECG. Conf Proc IEEE Eng Med Biol Soc 2007;1410–3.
17. Matavel A, Lopes CMB. PKC activation and PIP2 depletion underlie biphasic regulation of IKs by Gq-coupled receptors. J Mol Cell Cardiol 2009;46:704–12.
18. Matavel A, Medei E, Lopes CM. PKA and PKC partially rescue long QT type 1 phenotype by restoring channel-PIP2 interactions. Channels (Austin) 2010;4:3–11.
19. Locati EH, Zareba W, Moss AJ, et al. Age- and sex-related differences in clinical manifestations in patients with congenital long-QT syndrome—Findings from the international LQTS registry 11. Circulation 1998;97:2237–44.
20. Goldenberg I, Moss AJ, Peterson DR, et al. Risk factors for aborted cardiac arrest and sudden cardiac death in children with the congenital long-QT syndrome. Circulation 2008;117:2184–91.
21. Hobbs JB, Peterson DR, Moss AJ, et al. Risk of aborted cardiac arrest or sudden cardiac death during adolescence in the long-QT syndrome. JAMA 2006;296:1249–54.
22. Antzelevitch C, Shimizu W. Cellular mechanisms underlying the long QT syndrome. Curr Opin Cardiol 2002;17:43–51.
23. Antzelevitch C, Shimizu W, Yan GX, Sicouri S. Cellular basis for QT dispersion. J Electrocardiol 1998;30 Suppl:168–75.
24. Pajouh M, Wilson LD, Poelzing S, Johnson NJ, Rosenbaum DS. IKs blockade reduces dispersion of repolarization in heart failure. Heart Rhythm 2005;2:731–8.
25. Shimizu W, Antzelevitch C. Cellular basis for the ECG features of the LQT1 form of the long-QT syndrome: effects of beta-adrenergic agonists and antagonists and sodium channel blockers on transmural dispersion of repolarization and torsade de pointes. Circulation 1998;98:2314–22.
26. Antzelevitch C, Sun ZQ, Zhang ZQ, Yan GX. Cellular and ionic mechanisms underlying erythromycin-induced long QT intervals and torsade de pointes. J Am Coll Cardiol 1996;28:1836–48.
27. Zhu TG, Patel C, Martin S, et al. Ventricular transmural repolarization sequence: its relationship with ventricular relaxation and role in ventricular diastolic function. Eur Heart J 2009;30:372–80.
28. Yan GX, Antzelevitch C. Cellular basis for the normal T wave and the electrocardiographic manifestations of the long-QT syndrome. Circulation 1998;98:1928–36.
29. Yan GX, Shimizu W, Antzelevitch C. Characteristics and distribution of M cells in arterially perfused canine left ventricular wedge preparations. Circulation 1998;98:1921–7.
30. Zhu TG, Patel C, Martin S, et al. Ventricular transmural repolarization sequence: its relationship with ventricular relaxation and role in ventricular diastolic function. Eur Heart J 2009;30:372–80.
31. O'Hara T, Virag L, Varro A, Rudy Y. Simulation of the undiseased human cardiac ventricular action potential: model formulation and experimental validation. PLoS Comput Biol 2011;7:e1002061.
32. Fink M, Noble D. Markov models for ion channels: versatility versus identifiability and speed. Philos Transact A Math Phys Eng Sci 2009;367:2161–79.
33. Vincent GM, Jaiswal D, Timothy KW. Effects of exercise on heart rate, QT, QTc and QT/QS2 in the Romano-Ward inherited long QT syndrome. Am J Cardiol 1991;68:498–503.
34. Lane RD, Carmichael C, Reis HT. Differentiation in the momentary rating of somatic symptoms covaries with trait emotional awareness in patients at risk for sudden cardiac death. Psychosom Med 2011;73:185–92.
35. Barsheshet A, Goldenberg I, Uchi J, et al. Mutations in cytoplasmic loops of the KCNQ1 channel and the risk of life-threatening events: implications for mutation-specific response to beta-blocker therapy in type-1 long QT syndrome. Circulation 2012;125:1988–96.
36. Jons C, Moss AJ, Lopes CMB, et al. Mutations in conserved amino acids in the KCNQ1 channel and risk of cardiac events in type-1 Long QT syndrome. J Cardiovasc Electrophysiol 2009;20:859–65.

INTERNAL MEDICINE

Peripartum Cardiomyopathy Presenting with Syncope due to Torsades de Pointes: a Case of Long QT Syndrome with a Novel KCNH2 Mutation

Orie Nishimoto[1], Morihiro Matsuda[1,3], Kei Nakamoto[1], Hirohiko Nishiyama[1],
Kazuya Kuraoka[2], Kiyomi Taniyama[2,3], Ritsu Tamura[1],
Wataru Shimizu[4] and Toshiharu Kawamoto[1]

Abstract

Peripartum cardiomyopathy (PPCM) is a cardiomyopathy of unknown cause that occurs in the peripartum period. We report a case of PPCM presenting with syncope 1 month after an uncomplicated delivery. Electrocardiography showed Torsades de pointes (TdP) and QT interval prolongation. Echocardiography showed left ventricular systolic dysfunction and endomyocardial biopsy showed myocyte degeneration and fibrosis. Administration of magnesium sulfate and temporary pacing eliminated recurrent TdP. Genetic analyses revealed that recurrent TdP occurred via electrolyte disturbance and cardiac failure due to PPCM on the basis of a novel mutation in KCNH2, a gene responsible for inherited type 2 long QT syndrome.

Key words: Torsades de pointes, long QT syndrome, peripartum cardiomyopathy

Introduction

Peripartum cardiomyopathy (PPCM) is a disease of unknown cause that occurs from 1 month antepartum to 5 months postpartum in women without preexisting heart disease (1). In most cases, PPCM presents with signs of congestive heart failure caused by severe left ventricular (LV) systolic dysfunction. A few reported cases of PPCM have featured monomorphic ventricular tachycardia (VT) (2), but no cases have shown polymorphic VT.

Torsades de pointes (TdP), a polymorphic ventricular tachycardia associated with QT interval prolongation, is a life-threatening arrhythmia that can degenerate to fatal ventricular fibrillation. Acquired QT interval prolongation can occur upon exposure to environmental stressors such as particular classes of drugs, electrolyte disturbance, heart block,

or heart failure (3). Moreover, in patients with drug-induced acquired long QT syndrome (LQTS), mutations have been identified in genes encoding cardiac ion channels, such as KCNQ1, KCNH2, and SCN5A, which have proven to be associated with congenital LQTS. Here, we report a rare case of PPCM presenting with recurrent syncope due to TdP resulting from a KCNH2 mutation.

Case Report

A 33-year-old woman was admitted to our hospital with repeated syncope and seizures 1 month after an uncomplicated delivery. She did not have a history of pregnancy-associated diseases, spontaneous abortion or epilepsy or any symptoms of infectious disease or heart failure during pregnancy or after delivery. Prior to this pregnancy she had a delivery without any complications, and had no family history

461

Figure 1.　Electrocardiogram obtained at the time of syncope and seizure.
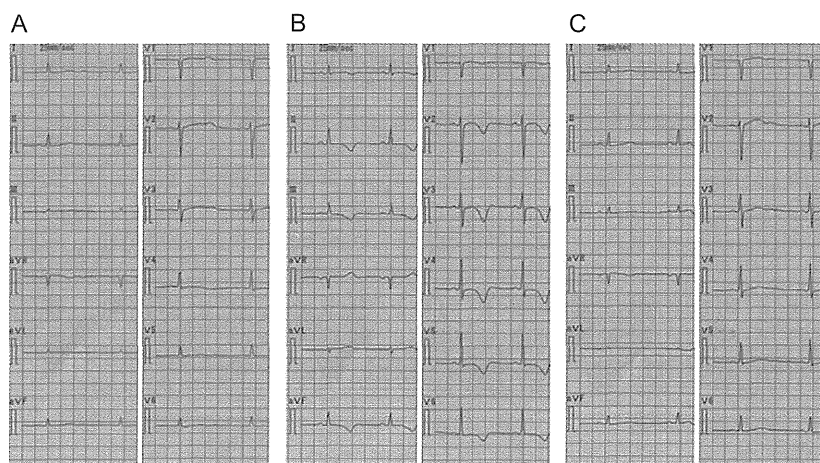
	Day 1	Day 8	Day 120
QTc (ms)	574	516	454
Blood Pressure (mmHg)	134/83	109/75	99/70
Heart Rate (bpm)	52	64	54
K (mEq/L)	3.4	4.4	4.2
Mg (mEq/L)	1.8	ND	ND

ND; not determined.

Figure 2.　Changes in electrocardiographic findings. Electrocardiograms obtained on admission (A), at day 8 (B), and at day 120 (C). QTc, blood pressure, heart rate, and K and Mg levels on the indicated day (D).

of heart disease or sudden death. Syncope and seizures had occurred a day before admission and the next morning and evening prior to admission, and then she was taken to the emergency room in our hospital. She had taken no medicine before admission.

The patient was alert upon admission, and the following vital signs were noted: blood pressure, 134/83 mmHg; pulse rate, 50 bpm; and body temperature, 36.7℃. The patient's height and weight were 158 cm and 50 kg, respectively. Physical examination did not reveal any signs of heart failure or abnormal neurological findings. Electrocardiography (ECG) showed sinus bradycardia (50 bpm) and marked QT

prolongation (QTc 574 ms) (Fig. 1, 2A). The chest X-ray image revealed a normal cardio-thoracic rate (48%) without pulmonary congestion or pleural effusion. Echocardiography showed impaired LV motion with mild hypokinesis at the base and severe hypokinesis at the apex. Laboratory data showed an elevated level of white blood cells (15,600/μL), mild elevation in the levels of brain natriuretic peptide (BNP) (123.1 pg/mL), hypokalemia (K levels, 3.4 mEq/L), and hypomagnesemia (Mg levels, 1.8 mEq/L), and normal serum levels of transaminases and creatinine. The levels of autoantibodies and viral antibodies were not significantly elevated, and the brain computed tomography image did not
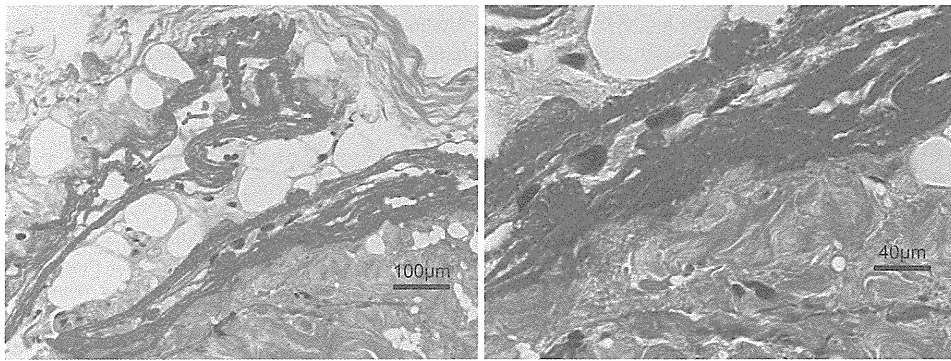
462

Figure 3.   Endomyocardial biopsy revealing cardiomyopathy. Masson's trichrome stain.

indicate any abnormalities.

She presented with syncope and seizures immediately after admission, and the ECG monitor indicated TdP (Fig. 1) that spontaneously ceased in 10-20 s. In spite of intravenous administration of magnesium sulfate (166 mEq), TdP recurred twice within a few hours. Correction of hypokalemia and temporary pacing at a rate of 80 bpm effectively inhibited the repeated syncope caused by TdP. She was administered 2.5 mg/day of enalapril after admission. After day 11, TdP did not recur even after discontinuation of temporary pacing. The patient was discharged on day 23.

On day 3, left ventriculography showed mildly impaired LV wall motion with an ejection fraction of 43.6%, although coronary angiography revealed no significant stenosis in the coronary arteries. Endomyocardial biopsy of the right ventricle revealed myocytes degeneration and interstitial fibrosis (Fig. 3). Follow-up ECGs showed that the positive or flat T wave in the leads I, II, III, aVF, and V2-6 was inverted until day 8, and then gradually returned to the up-right or flat form on day 120 (Fig. 2A-C). Prolonged QTc was shortened to 516 ms on day 8 and 454 ms on day 120 (Fig. 2D). Follow-up echocardiography on day 120 showed that LV contraction was almost normal.

Genetic analyses of KCNQ1, KCNH2, and SCN5A in this patient revealed a novel mutation in the KCNH2 gene. This mutation involved an insertion of AGGC at exon 11 (c.2680_2681), leading to a frameshift from R894, which results in a C-terminal truncating mutation (p.R894fsX920) in KCNH2. This mutation was also identified in her mother and sister, resulting in border range QTc (mother, 467 ms; and sister, 461 ms) without any episodes of syncope. Her mother had experienced three uncomplicated deliveries and one spontaneous abortion, and her sister had not experienced pregnancy.

Discussion

PPCM is relatively rare, with a currently accepted estimate of an incidence of approximately 1 per 3,000 to 1 per 4,000 live births in the United States, but it can be life-threatening, with mortality rates between 18% and 56% (1).

The present patient met the following 4 criteria for the diagnosis of PPCM, which was established by Demakis and Rahimtoola and others: 1) development of cardiomyopathy within 5 months of delivery, 2) absence of an identifiable cause of cardiomyopathy, 3) absence of recognizable heart disease before the last month of pregnancy, and 4) left ventricular systolic dysfunction with left ventricular ejection fraction (LVEF) of <45% (1, 4). Furthermore, histological investigation of the endomyocardial biopsy revealed myocyte degeneration and interstitial fibrosis, which may support the diagnosis of PPCM.

This PPCM patient showed recovery of ventricular function within 4 months after onset of syncope (5 months postpartum). Elkayam et al reported that recovery of LVEF (>50%) was observed in 54% of patients, and occurred within 6 months postpartum in most patients, which is distinct from other forms of non-ischemic cardiomyopathy. An improvement in LVEF at the last follow-up is significantly larger in women with an LVEF of >30% at time of diagnosis (5). For this reason, the present patient whose initial LVEF was 43.6% would be considered to be in a favorable position for spontaneous recovery. Similar to the medical management of patients with other forms of cardiomyopathy, ACE inhibitors and/or beta-blockers are commonly used for PPCM. Apart from the hemodynamic benefits of these classes of drugs, they may have the additional benefit of decreasing an overactive immune system, which plays a role in the basic pathophysiology of PPCM (6). Thus, the treatment of this patient with enalapril, an ACE inhibitor, from the first day after admission may have facilitated the improvement in PPCM.

The KCNH2 gene encodes the α-subunit of the voltage-gated potassium ion channel (Kv11.1, also called hERG), which plays a crucial role in ventricular repolarization. The role of KCNH2 is of particular pathophysiological importance, because mutations in this gene have been linked to the inherited type 2 long QT syndrome (LQT2) (3). We identified a novel KCNH2 gene mutation in the present patient and in 2 of her family members. This mutation was a 4-bp insertion leading to a C-terminal truncation of the hERG channel. Choe et al reported that functional assays

463

with 3 C-terminal truncating mutations in KCNH2 identified in the LQT2 families suggests an impaired ability of C-terminally truncated hERG protein to regulate channel activity in response to β-adrenergic stimulation (7). Based on their findings, we suspect that this novel mutation producing a truncated hERG protein at amino acid 920 should have a similar effect, although the functional effect of this mutation has not yet been clarified in vitro. Mild electrolyte abnormalities and cardiac failure due to PPCM led to marked QTc prolongation, and both the patient's QTc after recovery and those of her family members carrying this mutation were slightly prolonged (within border range), a finding that could be partly explained by this KCNH2 mutation. However, nevertheless, the patient's first delivery was uneventful, and her mother and sister were clinically unaffected by this mutation. Based on these facts, this mutation does not appear to have a strong impact on the phenotype of LQTS.

Women with LQT2, even without PPCM, are at increased risk for cardiac events during the postpartum period (8). However, it is difficult to predict cardiac events when such genetic mutations are not identified. Therefore, we recommend that the QT interval be measured in every pregnant woman, even those without preexisting cardiac diseases or a history of syncope to help prevent cardiac events, i.e., by avoiding hypokalemia and hypomagnesemia. In conclusion, we encountered a rare case of PPCM with recurrent syncope due to TdP. In this patient, inherited LQTS with KCNH2 mutation was unmasked via exposure to electrolyte disturbance and structural cardiac failure due to PPCM.

The authors state that they have no Conflict of Interest (COI).

References

1. Pearson GD, Veille JC, Rahimtoola S, et al. Peripartum cardiomyopathy: National Heart, Lung, and Blood Institute and Office of Rare Diseases (National Institutes of Health) workshop recommendations and review. JAMA **283**: 1183-1188, 2000.
2. Gemici G, Tezcan H, Fak AS, Oktay A. Peripartum cardiomyopathy presenting with repetitive monomorphic ventricular tachycardia. Pacing Clin Electrophysiol **27**: 557-558, 2004.
3. Roden DM, Viswanathan PC. Genetics of acquired long QT syndrome. J Clin Invest **115**: 2025-2032, 2005.
4. Demakis JG, Rahimtoola SH. Peripartum cardiomyopathy. Circulation **44**: 964-968, 1971.
5. Elkayam U, Akhter MW, Singh H, et al. Pregnancy-associated cardiomyopathy: clinical characteristics and a comparison between early and late presentation. Circulation **111**: 2050-2055, 2005.
6. Godsel LM, Leon JS, Engman DM. Angiotensin converting enzyme inhibitors and angiotensin II receptor antagonists in experimental myocarditis. Curr Pharm Des **9**: 723-735, 2003.
7. Choe CU, Schulze-Bahr E, Neu A, et al. C-terminal HERG (LQT 2) mutations disrupt IKr channel regulation through 14-3-3epsilon. Hum Mol Genet **15**: 2888-2902, 2006.
8. Seth R, Moss AJ, McNitt S, et al. Long QT syndrome and pregnancy. J Am Coll Cardiol **49**: 1092-1098, 2007.